Conceptual Design Method for the Wing Weight Estimation of Strut-Braced Wing Aircraft

Gabriel P. Chiozzotto
German Aerospace Center (DLR)
Research Engineer
Bunsenstr. 10, 37073, Göttingen, Germany
Gabriel.PinhoChiozzotto@dlr.de

ABSTRACT

This paper presents a method for the wing weight estimation of strut-braced wing aircraft in conceptual design. The method is simple to implement and captures important effects for the design of high aspect ratio braced wings. Conventional aluminum design or composites can be considered. Aeroelastic divergence, aileron reversal and elastic effects on the wing lift distribution are accounted for with simple strip theory and beam stiffness matrices. The stiffness matrices are extended to include the strut reaction. A direct method is used for the strut and wing internal loads calculation. Comparison with Nastran results shows good accuracy in the prediction of aeroelastic effects and strut reaction. Design studies show potential to reduce the wing mass between 11% and 14% or increase the aspect ratio from 10 to 12 in comparison to a conventional wing.

1 INTRODUCTION

The strut-braced wing (SBW) aircraft concept offers the opportunity to reduce the fuel consumption in comparison to conventional aircraft. This occurs due to the synergy of many positive effects: reduced vortex drag achieved with longer span, low wing weight, increased wing laminar flow and reduced wing sweep with thinner airfoils. Early studies and designs back to 1950 such as the Hurel-Dubois aircraft [1] already considered the advantages of braced wings. Despite its potential to reduce fuel consumption, the concept still has not found application in the large transport airplanes industry. Current goals for more environmental friendly aircraft [2] are encouraging new studies of the concept.
One of the main uncertainties of the design is related to the wing and strut weight. Due to the unconventional characteristics of the SBW, design-sensitive wing weight estimation methods must be developed to perform reliable feasibility studies. In this context, a method is presented here for application in conceptual design. It is flexible and simple to implement. It can be easily used in design studies and is sensitive to main design parameters taking into account the effects of the strut reaction and aeroelasticiy.

1.1 Previous work

The estimation of the wing weight and performance of SBW aircraft has been an important topic of research in different past and present activities. Research work has been taken around 1980 in a wide range of applications including regional turboprop [3], business jets [4], high-altitude research aircraft [5] and large military transports [6]. Research has been also performed at the Virginia Tech since many years (e.g. early work from 1998 [7] and more recently [8]). Recent research activities include the Boeing SUGAR project [9] and [10], research at ONERA [11], and the MIT [12]. In all cases methods have been developed to estimate the wing and strut weight. Most of the approaches are design oriented, developed to assist conceptual studies of the complete aircraft configuration. Some of the features common to most methods include: 1) structure sizing with classical wingbox station analysis; 2) rigid aerodynamic loads distribution either with vortex lattice methods (VLM) or analytical methods; 3) different approaches for the strut reaction ranging from Finite Element Methods (FEM) to simple assumptions and 4) symmetric maneuvers and taxi/landing cases. Although in many cases some aeroelastic analysis is performed, they are not considered directly in the wing sizing.

1.2 Requirements and objective

Based on the previous work, the following characteristics are important for the development of the current method: direct consideration of aeroelastic effects in the sizing and identification of a simple and effective strut reaction estimation method. It is also of importance to consider composites materials and the influence of gust loads on the high aspect ratio wings expected for the SBW.

The method must be suitable for conceptual design studies. Therefore, the following geometric design variables are of importance: wing loading, aspect ratio, airfoil thickness to chord ratio, wing sweep, wing taper and strut position. These are typical high level variables in early aircraft sizing. It is assumed that no information is yet available about: wing twist distribution, detailed airfoil geometry, detailed mass properties and structural arrangement. To be flexible in the application to new studies the method should be mostly analytical based and simple to implement, avoiding complex software implementation and debugging.

Considering these requirements, the following definitions set the scope of the current method: 1) analytical aerodynamics; 2) symmetric maneuver, taxi, Pratt gust and roll maneuvers load cases; 3) strut reaction calculation with analytical methods; 4) cross-section analytical sizing; 5) inclusion of aeroelastic effects and 6) consideration of composites materials using simple methods such as the ten-percent rule [13]. Moreover, the method should not only be capable of direct sizing but also optimizing structural design variables such as cover thickness, skin/stringer ratio and composite laminate arrangement. This should provide flexibility in the application for different types of studies.

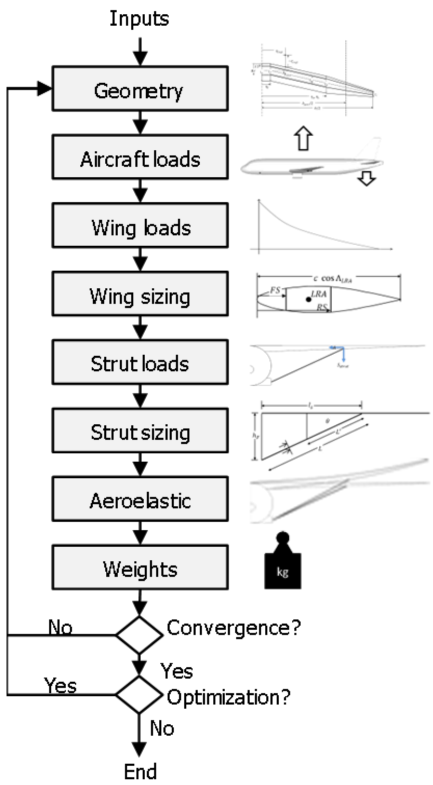

Figure 1: Method steps overview.

2 METHOD DESCRIPTION

The method developed requires a few input parameters and consists of the steps shown in Figure 1. Each step is described in detail in the following sections. The method is compact and can be implemented in a single Microsoft Excel worksheet.

Three solution sequences can be performed:

1. **Direct**: a direct non-iterative calculation with assumed initial wing mass for inertia relief and no corrections for aeroelasticity on the loads;
2. **Convergence**: the direct method is iterated until convergence of the initial wing mass (used for inertia relief) and aeroelastic corrections on the wing $C_{L\alpha}$ and lift distribution;
3. **Optimization**: involves convergence of the mass and aeroelastic corrections and additionally controls the covers and web thickness variables to meet aileron reversal and divergence requirements. The skin/stringer ratio and ribs spacing are also included as design variables.

2.1 Geometry

The wing planform is defined by four sections: wing root at symmetry plane, fuselage attachment, wing kink, and wing tip. The geometry definitions are shown in Figure 2. Each section has different local chord, wingbox geometry (front spar, FS and rear spar, RS) and airfoil thickness ratio (t/c). A straight Load Reference Axis (LRA) defines the wing sweep and crosses all sections in the center of the wing box. The strut attachment coincides with the wing kink. The strut has the same sweep angle of the LRA. The angle between the strut and the wing (perpendicular to the LRA) is θ_{st}, which is given by the strut span position and fuselage height, h_F. The strut total length is L and additional braces (juries) can be added equally dividing the strut into segments of length L'.
Concentrated masses such as engines and landing gears are positioned with non-dimensional spanwise η and chordwise ξ coordinates.

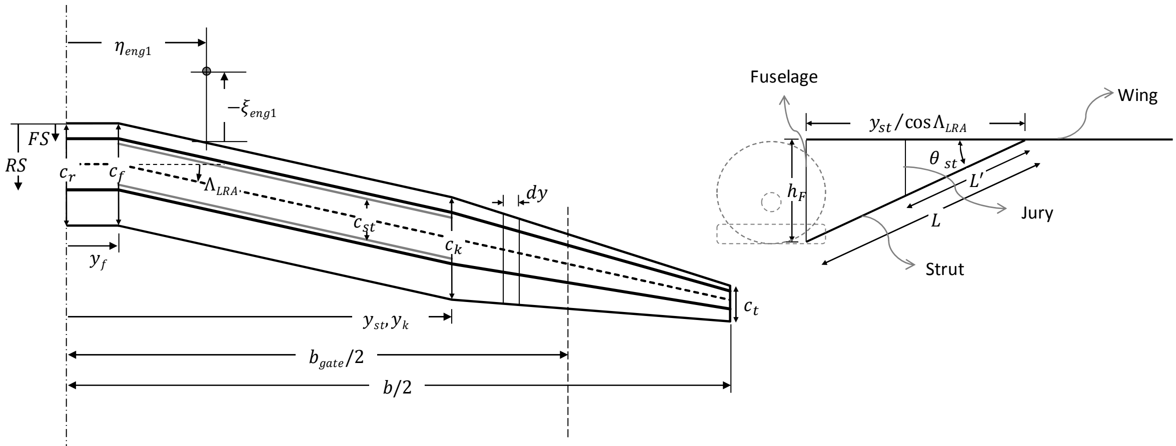

Figure 2: Basic geometry definitions.

2.2 Aircraft loads

Nine load cases expected to be critical for the wing and strut load carrying structures are considered as shown in Table 1. The maneuver speed VA is calculated assuming a maximum lift coefficient of 1.3. The cruise speed VC is equal to VMO, which is an input to the method. The dive speed is approximately $VD = VC + 25.6 m/s$ for a constant gravity acceleration in the upset maneuver from CS25.335(b)(1), ref. [14].
All cases with exception of the 1g fatigue case are considered to be limit loads with safety factors of 1.5 applied to the structure in the dimensioning. The fatigue case has a safety factor of 1.0. In all cases it is considered that the fuel mass is the difference between the case mass and the Maximum Zero Fuel Mass (MZFM).
The total loads acting on the aircraft consist of the wing lift (L_w), balancing tail load (BTL), inertia and loads due to the roll rate and aileron deflection. The wing lift and BTL are composed of 1g trim plus additional lift. This division is important because the 1g loads are distributed with an assumed flight shape lift distribution and the additional loads are calculated with aeroelastic effects:

$$\begin{aligned}\mathrm{BTL} &= \mathrm{BTL}_{1g} + \mathrm{BTL}_{\Delta} = \left[\frac{-m \cdot g \cdot (AC_{wb} - CG)}{l_t/MAC - AC_{wb} + 0.25}\right] + \left[\frac{-(n_z - 1) \cdot m\, g \cdot (AC_{wb} - CG)}{l_t/MAC - AC_{wb} + 0.25}\right] \\ \mathrm{L}_w &= \mathrm{L}_{w,1g} + \mathrm{L}_{w,\Delta} = \left(m\, g - \mathrm{BTL}_{1g}\right) + \left[(n_z - 1) m\, g - \mathrm{BTL}_{\Delta}\right]\end{aligned} \quad (1)$$

where m is the aircraft mass, g is the gravity acceleration, l_t is the distance from the tail 25% mean aerodynamic chord (MAC) to the wing 25%MAC and CG is the center of gravity position as a fraction of the wing MAC. The additional BTL_Δ is zero for the Pratt gust [15] cases since they represent non-balanced dynamic conditions. The wing-body aerodynamic center AC_{wb} (given as a fraction of the wing MAC) is calculated according to the semi-empirical methods from Torenbeek [16], which include the wing alone aerodynamic center and shifts due to the fuselage lift, wing lift loss over the fuselage and nacelles lift.

Table 1: Load cases considered for sizing.

Case	Aircraft mass	Design speed	Mach number	Load factor	Description	Possibly critical for
MA+	MTOM	VA	VA@0m	design (2.5)	low speed maneuver	covers, webs
MD+	MTOM	VD	MMO+0.07	design (2.5)	high speed maneuver	covers, webs
G+	MZFM	VC	MMO	Pratt	pos. gust	covers, webs
M-	MTOM	VC	MMO	-1.00	neg. maneuver	strut, lower panel
G-	MZFM	VC	MMO	Pratt	neg. gust	strut, lower panel
Bump	MTOM	-	-	1.67	bump on ground	strut, lower panel
1g	(MTOM+MZFM)/2	VC	MMO	1.00	fatigue case	lower panel
R+	MTOM	VC	MMO	1.67	steady roll rate	torsion wingbox
R-	MTOM	VC	MMO	0.00	steady roll rate	torsion wingbox

The wing lift coefficient derivative $C_{L\alpha}$ used in the gust cases is calculated with the following textbook equation [17] corrected for aeroelastic effects with the factor K_{el} (derived in section 2.7):

$$C_{L\alpha} = \frac{K_{el}\cdot 2\cdot\pi\cdot AR}{2+\sqrt{4+AR^2(1-MMO^2)\cdot[1+tan^2\Lambda_{LRA}/(1-MMO^2)]}} \tag{2}$$

where MMO is the maximum operating Mach number, which is also an input of the method.
A typical non-dimensional roll rate of $\hat{p} = pb/2V = 0.07$ is applied to the roll cases, including the required aileron deflection.

2.3 Wing loads

The distributed wing loading consists of the wing lift distribution and inertia relief due to the wing mass and fuel. The wing lift distribution is composed of three parts: 1g lift at flight shape, additional lift with elastic effects and lift due to roll case loadings (roll rate and aileron deflection):

$$ll_{aero,i} = \frac{c_{sch,i}}{K_I S} L_{w,1g} + \frac{k_{el,i}}{K_{el}}\frac{c_i}{K_I S} L_{w,\Delta} + \frac{1}{2}\rho_0 VMO^2\left(c_{sch,i}c_{l\hat{p},i}\hat{p} + c_{sch,i}c_{l\delta,i}\delta\right) \tag{3}$$

i is the station index, $c_{sch,i}$ is the local “Schrenk” chord (average between an equivalent elliptical wing and the actual planform [18]), c_i is the local planform chord, S is the wing planform area and $k_{el,i}$ is a factor to account for the aeroelastic effects (derived in section 2.7). In a direct solution sequence $k_{el,i} = 1$ for all wing stations corresponding to a rigid lift distribution. A correction factor for the lift loss over the fuselage (K_I) increases the loading to compensate for the reduced lift over the fuselage. The terms $c_{l\hat{p},i}\hat{p}$ and $c_{l\delta,i}\delta$ represent the local lift coefficients due to the roll rate and aileron deflection, both calculated with strip theory. ρ_0 is the air density at sea level.

For the lift loading, a vortex lattice method (VLM) could be used instead of the analytical strip-theory (Schrenk and planform). The strip-theory is nevertheless easy to implement and gives satisfactory results for early estimates.
All aileron derivatives (also for aileron reversal) are calculated with the thin airfoil theory as presented by Schlichting and Truckenbrodt [19] with corrections for sweep and Mach number:

$$\begin{aligned} c_{l\delta,i} &= C_{L\alpha}\left\{-\tau + k_{ail}\left[-\frac{2}{\pi}\left(\sqrt{\tau(1-\tau)} + \sin^{-1}\sqrt{\tau}\right) + \tau\right]\right\} \\ c_{m\delta,i} &= \frac{\cos^3 \Lambda_{LRA}}{\sqrt{1-Ma^2}} k_{ail}\left[-2\sqrt{\tau(1-\tau)^3}\right] \end{aligned} \tag{4}$$

where $\tau = c_{aileron}/c$ is the aileron chord to local chord ratio and k_{ail} is an effectiveness factor to calibrate the theoretical results to real conditions (a value of 0.75 is recommended).
The distributed inertia relief loading from the wing structure and fuel mass is proportional to the local volume:

$$ll_{inertia,i} = \frac{c_i^{\,2}(t/c)_i}{\sum c_i^{\,2}(t/c)_i\,\Delta y}\;(-n_z\,g)\left(m_{wing} + m_{fuel}\right) \tag{5}$$

where c_i is the local planform chord, $(t/c)_i$ is the local airfoil thickness to chord ratio, Δy is the station width, and m_{wing} and m_{fuel} are the wing and fuel masses respectively. The distribution proportional to the local volume according to Shanley [20] is a good approximation for the wing inertia distribution and also closely approximates the real fuel distribution.

Wing internal loads

The wing internal loads are calculated by integration of the distributed loading including also concentrated loads such as engines and landing gear reaction. Vertical shear, bending moment and torsion loads are considered.
The wing part inboard of the strut forms a statically indeterminate structure if no pinned wing connection is assumed at the fuselage. Therefore solving for the internal loads requires the stiffness distribution to be known in order to apply additional deflection constraints. At this step, no information is yet available about the stiffness distribution. One can then either use an iterative method (e.g. [6] and [7]) or assume a simplified strut reaction as in [9] and [12].
A direct approach similar to the one from [12] is applied here: it is assumed that all wing sections inboard of the strut are subject to the shear, bending moment and torsion moment at the strut attachment as shown in Figure 3. This method is easy to implement and presents a conservative approach since for a constant inboard planform also a constant inboard stiffness distribution is achieved. The constant inboard stiffness distribution is reasonable to account for stiffness (aeroelastic) and wing buckling requirements which could be significant if very low stiffness were allowed in this region. The very low stiffness would be typically obtained if the exact bending moment distribution with the strut relief was used for the sizing.
It is assumed that no axial loads caused by the strut act on the wing. This is justified for the wing upper cover if the strut is assumed to be attached to the lower cover. The axial load acting on the lower cover

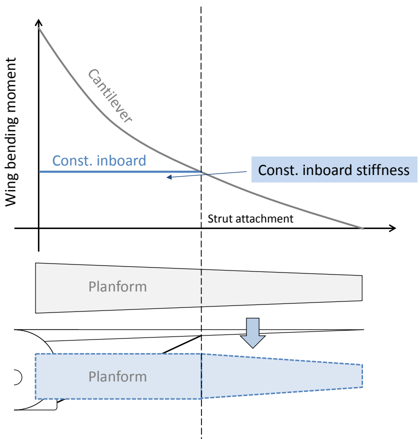

Figure 3: Constant inboard loading assumption.

induces a bending moment that reliefs exactly the additional axial loading on the upper cover. Neglecting the axial load on the lower cover is a conservative assumption since it reliefs the actual loading due to the bending moment.

2.4 Wing load carrying structure sizing

The wing load carrying structure is represented by a typical box beam section with smeared stringers as presented in Figure 4. The box width is given by the spar positions FS and RS. The box height is derived from the airfoil thickness equations of the NACA 4-digits airfoils with a reduction factor to account for the skin thickness [21]. The spar webs, upper/lower covers and ribs are sized at different stations over the wing for each load case. It is assumed that the webs carry shear and torsion, the covers carry bending and torsion and the ribs distribute the local shear forces. The webs and ribs are sized for strength and minimum thickness requirements while the covers are also sized for buckling and fatigue.

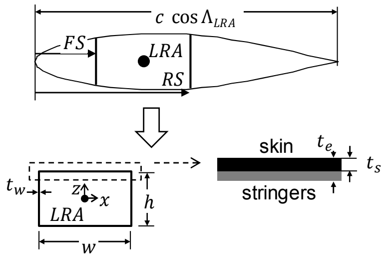

Figure 4: Wingbox geometry.

The upper and lower covers have different thicknesses but similar sizing equations. The sizing equations for their smeared thickness (t_e) are:

$$t_e = k_e k_{NO,e} \max\left(t_{e,buck}, t_{e,strength}\right) \tag{6}$$

$$t_{e,buck} = (P/w)/F_b \tag{7}$$

$$t_{e,strength} = \begin{cases} \sqrt{(P/w)^2 + 3(Q/k_s)^2}/F_{mat,t} \text{ , } if\ aluminum \\ \max\left((P/w)/F_{mat,t}, (Q/k_s)/F_{mat,s}\right) \text{ , } if\ composite \end{cases} \tag{8}$$

$$P = SF \cdot M_{LRA}/h \tag{9}$$

$$Q = SF \cdot T_{LRA}/(2 \cdot w \cdot h) \tag{10}$$

Where SF is the load case safety factor, P is the load on the cover panel due to the bending moment (M_{LRA}), Q is the shear flow due to the torsion moment (T_{LRA}), F_b is the buckling allowable, k_s is the skin/(skin+stringer) thickness ratio $k_s = t_s/\left(t_s + t_{stringer}\right)$, $F_{mat,t}$ is the material tensile allowable for ultimate loads (or fatigue allowable for 1g case), and $F_{mat,s}$ is the material shear allowable for ultimate loads. The factor k_e is a design variable (at each station) in the optimization problem to meet divergence and aileron reversal requirements. $k_{NO,e}$ is a non-optimal factor to account for missing load cases, simplified geometry representation and not modelled effects such as warping loads.

The required thickness for strength requirements in Eq. (8) considers different criteria for aluminum and composites. For aluminum materials the von Mises failure criterion is applied. For composites the failure criterion as presented by Hart-Smith in the ten-percent rule [13] is applied.

The sizing equations for the spar webs (t_w), ribs webs ($t_{rib,w}$) and ribs caps ($t_{rib,c}$ smeared over the rib depth h) thicknesses are:

$$t_w = k_w k_{NO,w} \frac{SF}{0.8\, F_{mat,s}} \left(\frac{|S_{LRA}|}{2h} + \frac{|T_{LRA}|}{2wh}\right) \tag{11}$$

$$t_{rib,w} = k_{NO,rib} \frac{SF \cdot ll_{aero} \cdot L_r \cos \Lambda_{LRA}}{h \cdot F_{mat,s}} + 0.003h \tag{12}$$

$$t_{rib,c} = 2\, k_{NO,rib} \frac{1}{h \cdot F_{mat,t}} \cdot \frac{SF \cdot ll_{aero} \cdot L_r \cos \Lambda_{LRA} \cdot w}{8} \cdot \frac{1}{h} \tag{13}$$

where S_{LRA} is the shear load at the station, L_r is the rib spacing (along the LRA), and dy is the section width as shown in Figure 2. The factor k_w is a design variable (at each station) in the optimization problem to meet divergence and aileron reversal requirements. $k_{NO,w}$ and $k_{NO,rib}$ are non-optimal factors to account for missing load cases and not modelled effects. The web factor 0.8 accounts in a simplified way for web buckling. The ribs webs term $0.003h$ is derived from [20] for webs and accounts for buckling.
The maximum thicknesses from all load cases and sizing criteria are selected as the final value at each station. The bending (EI_{xx}) and torsional stiffness (GJ) of the wingbox are calculated analytically at each station. The load carrying weight of covers, webs and ribs is given by:

$$m_{covers} = 2 \int_{y_f}^{b/2} (\rho_{up} t_{e,up} + \rho_{low} t_{e,low}) w \frac{dy}{\cos \Lambda_{LRA}} + 2\, (\rho_{up} t_{e,up} + \rho_{low} t_{e,low}) w\, y_f \big|_{y_f} \tag{14}$$

$$m_{web} = 2 \int_{y_f}^{b/2} 2\, \rho_w t_w h \frac{dy}{\cos \Lambda_{LRA}} + 4\, \rho_w t_w h\, y_f \big|_{y_f} \tag{15}$$

$$m_{rib} = 2 \int_{y_f}^{b/2} \rho_w (t_{rib,w} + t_{rib,c}) \frac{w\, h}{L_r} \frac{dy}{\cos \Lambda_{LRA}} + 2\, \rho_w (t_{rib,w} + t_{rib,c}) \frac{w\, h}{L_r}\, y_f \Big|_{y_f} \tag{16}$$

where ρ is the material density for each wingbox component.

Buckling allowable
The consideration of buckling requirements in preliminary sizing is complicated by the fact that not much information is available about the structure. The method considered here is an extension of the Farrar [22] method to account for different skin/stringer ratios. The buckling allowable for simultaneous skin and panel buckling is given by:

$$F_b = k_{comp} F(k_s) \sqrt{\frac{P}{w L_r} E_{x0}} \tag{17}$$

but instead of using the typical maximum $F(k_s)$ for different stringers (e.g. 0.95 for Z-section), a curve fit from the Z-stringer chart presented by Farrar is used:

$$F(k_s) = 0.90(1 - 0.00617 e^{5.0449 k_s}) \tag{18}$$

This equation allows for skin/stringer ratios which are different than the optimum for buckling to be considered. The factor 0.90 accounts for the maximum practical realized values as suggested by Farrar. The equation is valid for skin/(skin+stringer) ratios of $0.40 \leq k_s \leq 0.86$. The composite factor $k_{comp} = 0.725 \cdot Z^{1/4}$ is used to account for composites as developed by Tetlow [23] where Z is:

$$Z = \frac{E_x}{(E_{x0})^2} \frac{\pi^2}{6(1-\mu_{xy}\mu_{yx})} \left[(E_x \cdot E_y)^{1/2} + \frac{\mu_{xy}E_y}{2} + \frac{\mu_{yx}E_x}{2} + 2(1-\mu_{xy}\mu_{yx})G_{xy} \right] \tag{19}$$

E_{x0} is the ply longitudinal modulus and E_x, E_y, G_{xy}, μ_{xy} and μ_{yx} are the laminate properties calculated with the ten-percent rule [13].

2.5 Strut loads

With the wing load carrying structure stiffness properties available, it is possible to calculate the strut reaction for the statically indeterminate structure. The method considered here is similar to the one presented by Park [3]. The strut vertical reaction S_{st} is solved from the vertical deflection boundary condition at the wing-strut attachment. A rigid strut is assumed. Therefore it is not necessary to know the strut stiffness at this step:

$$\frac{S_{st}L}{A_{st}E_{st}} = z_w(y_{st}) + S_{st}\, z'_{st}(y_{st}) \Rightarrow \frac{S_{st}L}{A_{st}E_{st}} \approx 0 \Rightarrow S_{st} \cong -\frac{z_w(y_{st})}{z'_{st}(y_{st})} \tag{20}$$

where the vertical deflection of an equivalent cantilever wing z_w and the deflection due to a unit vertical force at the strut z'_{st} are:

$$\begin{aligned} z_w(y_A) &= \int_{y_f}^{y_A} \frac{dz_w}{dy} dy \text{ and } \frac{dz_w}{dy}(y_A) = \int_{y_f}^{y_A} \frac{M_{LRA}}{EI_{xx}} dy \\ z'_{st}(y_A) &= \int_{y_f}^{y_A} \frac{dz'_{st}}{dy} dy \text{ and } \frac{dz'_{st}}{dy}(y_A) = \int_{y_f}^{y_A} \frac{(y_{st}-y)/\cos\Lambda_{LRA}}{EI_{xx}} dy \end{aligned} \tag{21}$$

2.6 Strut sizing

The strut load carrying structure is a box with covers and spars in a construction similar to the wing. The strut is sized by buckling requirements only. No column buckling of the complete strut is allowed up to ultimate loads. The stiffness required to preclude buckling and the equivalent thickness of the covers are given by:

$$EI_{req} = SF \frac{max\, S_{st}}{\sin\theta_{st}} \frac{(L')^2}{\pi^2} \text{ and } t_{e,st} = max\left(\frac{EI_{req}}{E_{st}} \frac{2}{w_{st}h_{st}^2}, \frac{t_{min,st}}{0.5}\right) \tag{22}$$

where the strut length L' accounts for supporting juries as shown in Figure 2. w_{st} and h_{st} are the strut box dimensions. E_{st} is the strut material modulus of elasticity and $t_{min,st}$ is the strut minimum skin thickness. A skin/(skin+stringer) ratio of 0.5 is assumed. The thicknesses of the strut front and rear spar webs have the same thickness as the skin covers.

Sizing criteria for the juries are difficult to define since they depend on many different factors such as global buckling loads and indeterminate loads of a truss wing. Therefore in the present method the juries are simply represented by box structures with all dimensions equal to half of the strut dimensions (chord, box width, box height and box wall thickness). This adds a simple weight penalty for adding juries.

The stiffness properties (out of plane bending, $EI_{xx,st}$; in-plane bending, $EI_{zz,st}$ and torsion GJ_{st}) of the strut and juries are calculated from the thickness estimations above. The weight of the strut and juries box ribs is set to 15% of the weight from covers and webs. This is a typical value for wing boxes. The final weights of the load carrying strut and juries boxes are:

$$m_{st,box} = 2 \cdot 1.15 \cdot \rho_{st} \left[2\left(w_{st}t_{e,st} + 0.5h_{st}t_{e,st}\right)\right]L \tag{23}$$

$$m_{st,jury\ box} = 2 \cdot 1.15 \cdot \rho_{st} \left[2\left(\frac{w_{st}}{2}\frac{t_{e,st}}{2} + 0.5\frac{h_{st}}{2}\frac{t_{e,st}}{2}\right)\right]L' \sin\theta_{st} \tag{24}$$

2.7 Static aeroelasticity

Aeroelastic effects must be considered even in early weight estimations if flexibility effects are likely to be significant. This is the case of high aspect ratio, low stiffness wings expected in SBW concepts. A simple aeroelastic model capable of representing general design trades is developed for this purpose.

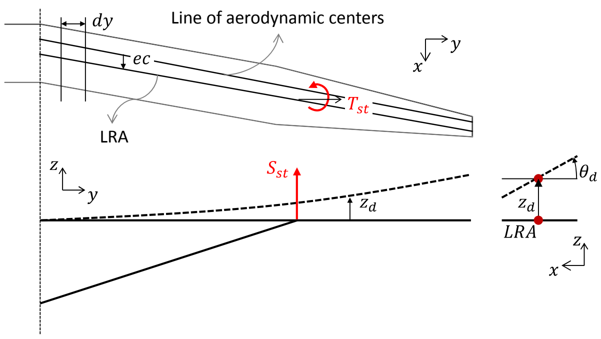

Figure 5: Aeroelastic model definitions.

The main aeroelastic effects of interest are: static aeroelastic effects on loads (gust response and aerodynamic load distribution) and aeroelastic stability requirements (flutter, divergence and aileron reversal). To keep the formulation simple no flutter analysis is included. The divergence and aileron reversal restrictions add a weight penalty for stiffness requirements.

The formulation and notation employed here follows the classical work from Bisplinghoff, Ashley, and Halfman [24]. The structure is represented by a simple swept beam and aerodynamics is modelled with the strip theory. This formulation allows the use of small matrices (approximately 10 by 10 elements) to represent the effects of interest. Relevant geometry definitions for the aeroelastic model are shown in Figure 5. Additional work developed within the scope of this paper includes the development and extension of the equations considering the strut reaction.

Aerodynamic and structural model

The aerodynamic influence coefficient matrix $[A]$ is diagonal according to the strip-theory. Its main diagonal elements are given by:

$$A_{ii} = \frac{1}{c_i C_{L\alpha}} \tag{25}$$

where $C_{L\alpha}$ is calculated using Eq. (2) with $K_{el} = 1$.

Table 2: Structural influence coefficients formulation [24].

Description	Equations
Deflection due to vertical force	$C^{zz}(y,\eta) = \int_{y_f}^{\min(y,\eta)} \frac{(\eta-\lambda)(y-\lambda)}{EI}\frac{d\lambda}{\cos^2\Lambda}$
Streamwise torsion due to torsion moment	$C^{\theta\theta}(y,\eta) = \int_{y_f}^{\min(y,\eta)} \left(\frac{\cos^2\Lambda}{GJ} + \frac{\sin^2\Lambda}{EI}\right)\frac{d\lambda}{\cos\Lambda}$
Streamwise torsion due to vertical force	$C^{\theta z}(y,\eta) = -\sin\Lambda \int_{y_f}^{\min(y,\eta)} \frac{(\eta-\lambda)}{EI}\frac{d\lambda}{\cos^2\Lambda}$

The structural model consists of a structural influence coefficient matrix representing the vertical $\{z_d\}$ and streamwise torsion $\{\theta_d\}$ deflections (see Figure 5) due to applied vertical forces $\{F_z\}$ and streamwise torsion moments $\{T_\theta\}$ at each station:

$$\begin{bmatrix} [C^{\theta\theta}] & [C^{\theta z}] \\ [C^{z\theta}] & [C^{zz}] \end{bmatrix} \begin{bmatrix} \{T_\theta\} \\ \{F_z\} \end{bmatrix} = \begin{bmatrix} \{\theta_d\} \\ \{z_d\} \end{bmatrix} \tag{26}$$

The structural influence coefficient matrix is partitioned into three matrices representing the vertical deflection due to vertical force $[C^{zz}]$, torsion due to torsion moment $[C^{\theta\theta}]$ and torsion due to vertical force coupling for swept wings $[C^{\theta z}]$. The equations used to calculate the elements of these matrices are presented in Table 2 and are adapted from [24]. They are derived from a simple swept wing with a straight beam axis. All integrals are evaluated numerically.

Aeroelastic equations for cantilever wing

The static aeroelastic equation for a cantilever wing neglecting airfoil pitching moments and inertia relief is given by:

$$([A] - q[E])\{cc_l\} = \{\alpha\} \text{ with } [E] = ([C^{\theta z}] + [C^{\theta\theta}][ec])[dy] \tag{27}$$

$\{cc_l\}$ is the vector of lift coefficients multiplied by the local chord at each strip, $\{\alpha\}$ is the vector of local angles of attack and $[E]$ is the structural flexibility matrix coupled to the aerodynamic strips. $[ec]$ is a diagonal matrix with the streamwise distances between aerodynamic centers and load reference axis (Figure 5). $[dy]$ is also a diagonal matrix with the streamwise width of each strip (Figure 5). q is the dynamic pressure.

Inclusion of strut reaction in the aeroelastic equations

The cantilever wing equations presented are extended to include the strut effect. The objective is to add a correction matrix $[K_E]$ to $[E]$ in Eq. (27) accounting for the strut torsion and vertical reaction.
The torsion at each strip due to the distributed lift $\{cc_l\}$ and pitching moment $\{c^2c_m\}$ coefficients plus the torsion due to the strut streamwise torsion moment and vertical force at the strut is:

$$q[E]\{cc_l\} + q[F]\{c^2c_m\} + [C^{\theta\theta}]\{1_{st}\}T_{st} + [C^{\theta z}]\{1_{st}\}S_{st} = \{\alpha\} \tag{28}$$

where $[F] = [C^{\theta\theta}][dy]$ is the structural flexibility matrix coupled to the aerodynamic pitching moment. $\{1_{st}\}$ is a column vector with 1 at the wing strip connected to the strut and zeros at the other strips. T_{st} is the strut streamwise torsion reaction and S_{st} is the strut vertical reaction as shown in Figure 5.
To keep the equations similar to the cantilever wing case, it is of interest to express T_{st} and S_{st} as functions of the wing aerodynamic loadings coefficients $\{cc_l\}$ and $\{c^2c_m\}$. This is achieved by writing the boundary conditions of equal torsion angle and vertical displacement at the wing strip connected to the strut:

$$\begin{aligned} T_{st}C_{ss}^{\theta\theta} + S_{st}C_{ss}^{\theta z} + q\{1_{st}\}^T([E]\{cc_l\} + [F]\{c^2c_m\}) = c_T T_{st} \;\Rightarrow\; T_{st}C_{ss}^{\theta\theta} + S_{st}C_{ss}^{\theta z} + A = c_T T_{st} \\ S_{st}C_{ss}^{zz} + T_{st}C_{ss}^{\theta z} + q\{1_{st}\}^T([E']\{cc_l\} + [F']\{c^2c_m\}) = c_S S_{st} \;\Rightarrow\; S_{st}C_{ss}^{zz} + T_{st}C_{ss}^{\theta z} + A' = c_S S_{st} \end{aligned} \tag{29}$$

$C_{ss}^{\theta\theta}$, $C_{ss}^{\theta z}$ and C_{ss}^{zz} are the wing structural influence coefficients at the wing strip connected to the strut due to loadings at the same strip. c_T and c_S are the torsional and vertical flexibility coefficients of the complete strut (to be developed later). $[E']$ and $[F']$ are similar to $[E]$ and $[F]$ but represent the vertical displacement (z_d) due to loading:

$$[E'] = ([C^{zz}] + [C^{\theta z}][ec])[dy] \text{ and } [F'] = [C^{\theta z}][dy] \tag{30}$$

After some manipulation of Eq. (29) we can express T_{st} and S_{st} as functions of A and A':

$$T_{st} = A \cdot B_{T1} + A' \cdot B_{T1'} \text{ and } S_{st} = A \cdot B_{S1} + A' \cdot B_{S1'} \tag{31}$$

where,

$$B_{T1} = -(C_{SS}^{zz} - c_S)/B \;;\; B_{T1'} = B_{S1} = C_{SS}^{\theta z}/B \text{ and } B_{S1'} = -\left(C_{SS}^{\theta\theta} - c_T\right)/B$$
$$B = (C_{SS}^{zz} - c_S)\left(C_{SS}^{\theta\theta} - c_T\right) - \left(C_{SS}^{\theta z}\right)^2 \tag{32}$$

Inserting Eq. (31) and Eq. (32) back into Eq. (28) we obtain:

$$q([E] + [K_E])\{cc_l\} + q([F] + [K_F])\{c^2c_m\} = \{\alpha\} \quad \Rightarrow \quad q[E_K]\{cc_l\} + q[F_K]\{c^2c_m\} = \{\alpha\} \tag{33}$$

where the correction matrices due to the strut reactions are:

$$[K_E] = \left[C^{\theta\theta}\right]\{1_{st}\}\{1_{st}\}^T([E]B_{T1} + [E']B_{T1'}) + \left[C^{\theta z}\right]\{1_{st}\}\{1_{st}\}^T([E]B_{S1} + [E']B_{S1'})$$
$$[K_F] = \left[C^{\theta\theta}\right]\{1_{st}\}\{1_{st}\}^T([F]B_{T1} + [F']B_{T1'}) + \left[C^{\theta z}\right]\{1_{st}\}\{1_{st}\}^T([F]B_{S1} + [F']B_{S1'}) \tag{34}$$

Eq. (33) is a convenient way of considering the strut reaction in the simple static aeroelastic equations from Bisplinghoff, Ashley, and Halfman [24]. Validation of this formulation is presented in section 3.2 with MSC Nastran [25] results.
The only remaining data are the flexibility coefficients c_T and c_S of the strut. They are calculated after some coordinate transformations from the strut coordinate system to the global coordinate system and are given by:

$$c_T = -1/\left(\frac{EI_{zz,st}}{L}\cos^2\Lambda_{LRA}\sin^2\theta_{st} + \frac{EI_{xx,st}}{L}\sin^2\Lambda_{LRA} + \frac{GJ_{st}}{L}\cos^2\Lambda_{LRA}\cos^2\theta_{st}\right)$$
$$c_S = -1/\left(\frac{A_{st}E_{st}}{L}\right) \tag{35}$$

Divergence speed, aileron reversal and aeroelastic effects on lift distribution
The divergence speed of the wing and strut is calculated by solving the aeroelastic equations for the lowest eigenvalue:

$$([A] - q[E_K])\{cc_l\} = 0 \tag{36}$$

The lift on the strut is neglected as being small in comparison to the lift on the wing. The aileron reversal speed is calculated iteratively according to [24]:

$$q_{rev} = -\frac{\lfloor H\rfloor\{cc_{l,\delta}{}^r\}}{\lfloor H\rfloor([A] - q_{rev}[E_K]])^{-1}\left([E_K]\{cc_{l,\delta}{}^r\} + [F_K]\{c^2c_{m,\delta}{}^r\}\right)} \tag{37}$$

where $\lfloor H\rfloor = \lfloor 1\rfloor\lceil y\rfloor\lceil dy\rfloor$ is a row vector that adds the rolling moment of each strip and the superscript r indicates rigid loadings calculated with Eq. (4).
All aerodynamic coefficients applied in the aileron reversal and divergence equations are calculated for a Mach number equal to the dive Mach number. It is then verified if the equivalent divergence and aileron reversal speeds are outside the aeroelastic stability envelope: $V_{rev}, V_{div} > 1.15 \cdot VD$ according to CS25.629.
The aeroelastic correction factors at each station for the lift distribution $k_{el,i}$ in Eq. (3) are calculated with the aeroelastic model at each of the design speeds VA, VC and VD for a unit increase in angle of attack:

$$([A] - q[E_K])\{cc_{l,\alpha}\} = \{1\} \text{ and } k_{el,i} = \left(cc_{l,\alpha}\right)_i/\left(cc_{l,\alpha}{}^r\right)_i \tag{38}$$

where $cc_{l,\alpha}{}^{r}$ is the rigid lift coefficient derivative, Eq. (2) with $K_{el} = 1$, multiplied by the local chord. Equation (2) is evaluated at the Mach number of the speed of interest (VA, VC or VD).
The total wing $C_{L,\alpha}$ elastic correction factor applied to Eq. (2) and Eq. (3) is then given by:

$$K_{el} = \frac{\sum \left(cc_{l,\alpha}\right)_i \Delta y_i}{\sum \left(cc_{l,\alpha}{}^{r}\right)_i \Delta y_i} \tag{39}$$

2.8 Wing weight

The total wing structural weight is the sum of the analytical estimations (wing and strut load carrying structures) and semi-empirical methods. Allowance for installation and assembly is accounted for in the wing covers, webs and ribs weights with the factors provided in [26] (+5% aluminum covers/ribs, +8% composite covers/ribs and +9% webs). An assembly factor of 15% is assumed for the strut. An overall allowance factor of 10% is still added to all analytical weight estimations to account for simplifications and other unexpected weight growths. Due to the importance of weight bookkeeping, a detailed description of the group weight definitions used in the present method is shown in Table 3.

Table 3: Wing group weight definitions.

Group weight	Components	Eq.	Calc.*
1 Wingbox			
1.1 Bending material			
1.1.1 Optimal	optimal wingbox load carrying upper and lower covers (skin+stringers), including additional material for stiffness requirements. Includes center wing box.	(14)	A
1.1.2 Non-optimal	covers correction due to non-optimal thickness, taper, joints and installation.	(40)	E
1.2 Webs	optimal wingbox spar webs (front and rear), including additional material for stiffness requirements and installation allowances. Includes center wing box.	(15)	A
1.3 Ribs	ribs webs and caps inside the wingbox including allowances for installation. Includes center wing box.	(16)	A
2 Secondary structure	movables (spoilers, ailerons, slats and flaps) including bodies, tracks, supports and attachments. Fixed LE and TE panels, ribs and assembly items. Fairings from: pylons, tracks and root. LG and pylons attachments, wingtip (incl. winglet), paint and miscellaneous.	(41)	E
3 Strut			
3.1 box optimal	optimal strut covers, webs and ribs to avoid buckling of the strut.	(23)	A
3.2 box non-optimal	covers correction due to non-optimal thickness, taper, joints and installation.	(42)	E
3.3 strut sec. structure	strut fixed LE and TE panels, ribs and assembly items.	(43)	A
3.4 jury	jury optimal box structure.	(24)	A
3.5 jury non-optimal	jury non-optimal structure.	(44)	A
3.6 jury sec. structure	jury fixed LE and TE panels, ribs and assembly items.	(45)	A
4 Folding	folding wing for airport gate restriction penalty.	(46)	E

*Calculation method: A – analytical plus correction factors, E – semi-empirical.

The remaining equations for the complete wing weight are:

$$m_{NO} = \rho_e S \left[1 + 2\left(\frac{t}{c}\right)_m\right] \delta_{NO} \tag{40}$$

$$m_{sec} = MTOM^{0.518} S^{0.492} \tag{41}$$

$$m_{NO,st} = \rho_{st}(2\, c_{st} L \cos \Lambda_{LRA}) \left[1 + 2\left(\frac{h_{st}}{c_{st}}\right)\right] \delta_{NO} \tag{42}$$

$$m_{sec,st} = 1.15 \cdot 2 \cdot \rho_{st}\left[2.1 L(c_{st} \cos \Lambda_{LRA} - w_{st}) t_{min,st}\right] \tag{43}$$

$$m_{NO,jury} = 0.5\, m_{st,jury} \tag{44}$$

$$m_{sec,jury} = 1.15 \cdot 2 \cdot \rho_{st}\left[2.1 L' \sin \theta_{st} \left(\frac{c_{st}}{2} \cos \Lambda_{LRA} - \frac{w_{st}}{2}\right) t_{min,st}\right] \tag{45}$$

$$m_{fold} = 0.042\, n_z\, MTOM\, \frac{1}{2}\left(1 - \frac{2}{\pi}(b_{gate}/b)\sqrt{1 - (b_{gate}/b)^2} - \frac{2}{\pi} \sin^{-1}(b_{gate}/b)\right) \tag{46}$$

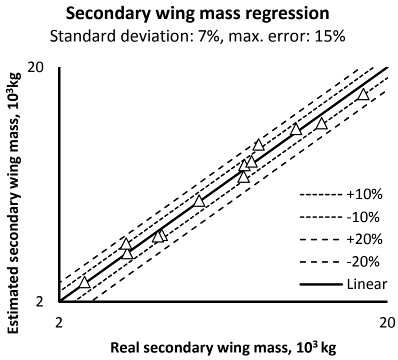

Figure 6: Secondary wing mass regression.

The non-optimal material Eq. (40) is presented in [27] and is also adapted to the strut in Eq. (42). The wing secondary structure Eq. (41) has been developed with data from 13 commercial aircraft from [28] and [29]. It is based on the rationale that most of the secondary structure components scale with the area and some with the take-off mass (flaps and pylon attachments). The regression is shown in Figure 6.
Since no data is available on actual SBW large commercial aircraft the strut secondary structure weight must be estimated with simplified equations based on the geometry. The weight of the fixed LE and TE of the strut (in front and behind of the strut wingbox) are given by a constant minimum thickness applied to the covers, Eq. (43). The factor 2.1 accounts for the airfoil curvature and exposed area while the factor 1.15 is an allowance for other additional weights (ribs and assembly items). The same equation is applied to the jury structure. The folding span weight penalty Eq. (46) for airport gate restrictions is an adaptation of the semi-empirical method from [8].

3 VALIDATION AND DESIGN STUDIES

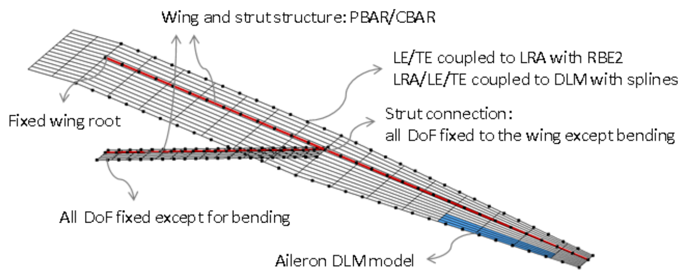

Figure 7: Example of Nastran model used for validation.

Validation of the present method is presented for three cases: internal loads comparison with Nastran, aeroelastic effects comparison with Nastran and wing mass estimation accuracy for conventional aircraft. For the validation studies with Nastran a representative short range SBW aircraft with $MTOM = 75{,}000\, kg$, $W/S = 5500\, N/m^2$ and $AR = 18$ is used. The strut chord is 25% of the wing chord at the kink location and the strut box corresponds to 30% of the strut chord. The wing is conventional metal construction and the strut is made of carbon fiber reinforced plastic (CFRP) of high longitudinal stiffness (laminate percentage of 0°/±45°/90° plies: [50/38/12]). The engines are located at the fuselage rear part. The Nastran models for validation are generated automatically as an output of the current method. An example is shown in Figure 7.

3.1 Internal loads comparison with Nastran

The purpose of this validation case is to verify two assumptions in the development of the current method: the constant inboard stiffness from section 2.3 and the direct calculation of the strut axial load from section 2.5. The distributed loading of a 2.5g maneuver case is applied to a Nastran beam model similar to Figure 7 (only stiffness model, no DLM) and the internal loads from Nastran are compared to the ones calculated with the current method. The results are shown in Figure 8 for four strut positions along the span: 0.2, 0.4, 0.6 and 0.8. Three strut constructions are evaluated: no jury, one jury and minimum strut cover panel thickness ($tmin$). The minimum strut cover thickness represents a limit case for the strut deflection. It is added as a worst case test for the assumption of no deflection at the strut attachment (section 2.5). The results for a statically determinate structure with a pinned wing root are also calculated and shown for reference.

Based on the results shown in the bending moment diagram it can be concluded that the assumption of constant inboard loading (section 2.3) is realistic and conservative. In most of the cases the bending moment inboard of the strut is lower than at the strut-wing attachment. The only exception is for strut attachments placed far outboard.

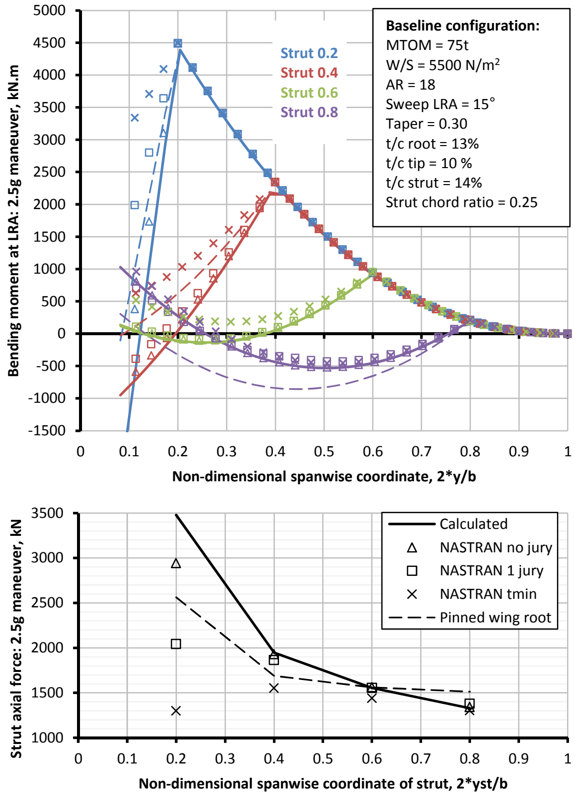

Figure 8: Internal loads validation with Nastran.

The strut axial force as a function of the strut spanwise position confirms the assumptions of section 2.5 in the calculation of the strut reaction. As expected, the calculated results accuracy increases with the stiffness of the strut (e.g. no jury). Good results are achieved even for struts with minimum cover thickness. The axial force is overestimated only for struts that are very close to the wing root. In this region the loads relief on the wing is likely to be very low and the SBW concept not advantageous.

3.2 Aeroelastic effects comparison with Nastran

This validation case is performed to verify the aeroelastic model developed in section 2.7. A Nastran aeroelastic model is automatically generated as shown in Figure 7. The divergence speed, aileron reversal and wing elastic $C_{L\alpha}$ are calculated with Nastran and compared with the results of the current method. The results for different sweep angles, aspect ratios, and strut positions of the baseline configuration are shown in Figure 9. The airfoil thickness to chord ratio is chosen for each sweep angle according to aerodynamic compressibility drag requirements. All configurations include one additional brace (jury).

The results compare favorably for most cases. Some higher deviations occur for aft sweep configurations with the strut at 70% of the wing span. The results also show the importance of considering aeroelastic restrictions. There is a decrease in divergence and aileron reversal speeds for struts placed increasingly outboard.

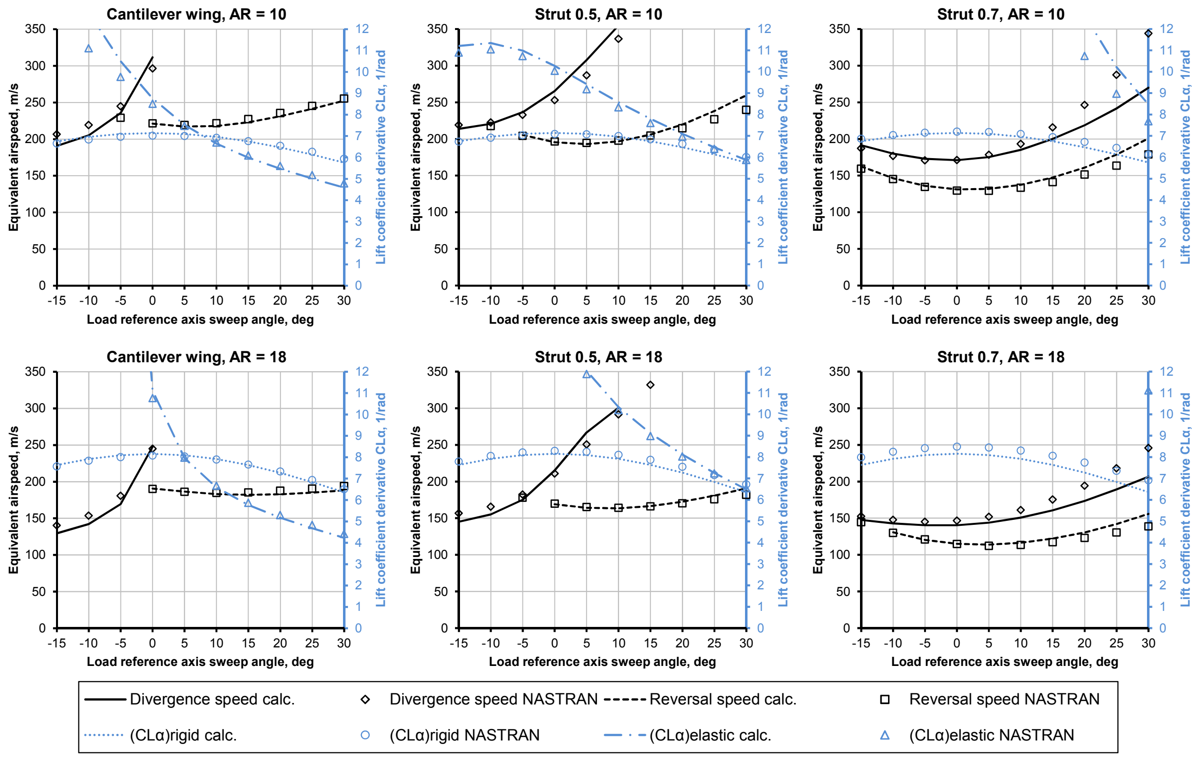

Figure 9: Aeroelastic results comparison with Nastran . The elastic CLα is calculated at V=165m/s, EAS.

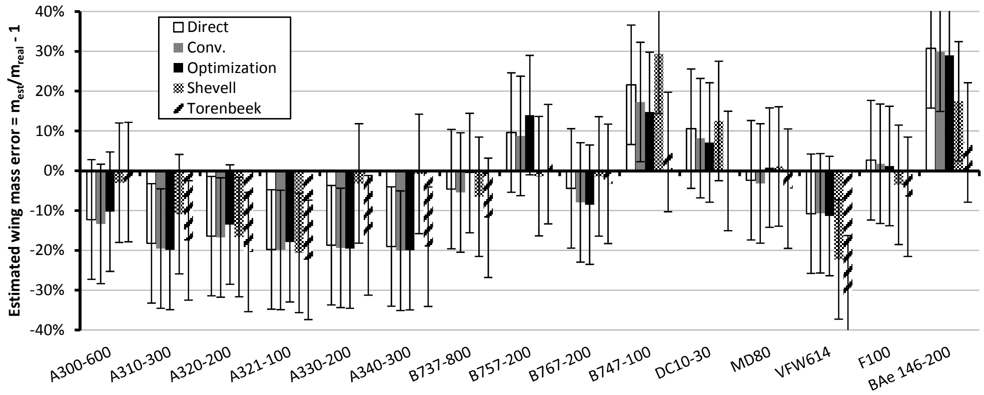

Figure 10: Conventional aircraft wing mass estimation error. Error bars indicate standard deviation of 15%.

3.3 Conventional aircraft wing mass estimation

Mass properties estimation of unconventional aircraft is a very difficult task since no historical data is available. Nevertheless it is also important to verify the accuracy of the current method to estimate the wing mass of conventional aircrafts. Therefore 15 commercial aircraft configurations are selected for validation. Geometry, weights, performance and other data are gathered from many sources including data published by the manufacturers, design books (ref. [16], [17] and [30]), LTH [31], design studies

with calibrated tools [32], and others. Thus some uncertainty regarding geometry definitions, group weight statements, and different design philosophies is present.
The current method is applied with the three different solution sequences: direct, convergence and optimization. Two other analytical methods (Shevell and Torenbeek) calibrated with historical data are used as reference for the accuracy. The estimated mass error for each aircraft is shown in Figure 10. All methods have standard deviations of about 15% with maximum absolute errors of 30%. This accuracy is acceptable considering the uncertainties in the available data and the typical expected errors in early design estimates. All methods agree well for all aircraft configurations within the standard deviation of 15%.

4 DESIGN STUDY: WING MASS AS A FUNCTION OF ASPECT RATIO

A design study is performed to illustrate the application of the current method. A similar short range aircraft configuration as used in the Nastran validation analyses is considered. The study consists in verifying the SBW concept potential in comparison with a conventional cantilever wing for increasing aspect ratio. All other main design parameters (wing loading, MTOM, sweep angle and average t/c) are kept constant. The wing weight is estimated for each concept (SBW and conventional) with rigid wing loads, elastic wing loads and optimization to meet aeroelastic requirements (divergence and aileron reversal). Typical aluminum construction is also compared with CFRP for each case. The T300-5208 [33] is used as baseline for the CFRP laminates. Three laminates are considered for the upper and lower covers of the wingbox: [50/38/12], [40/48/12], [30/58/12]. The webs and ribs laminates are fixed at [12/76/12]. The strut is made of [50/38/12] laminates for both the aluminum and CFRP constructions.
The results are shown in Figure 12. The SBW results correspond to the minimum weight strut spanwise position as shown in Figure 11. The strut position is limited to the range between 30% and 65% of the semi-span. The composite results correspond to the minimum weight laminate from the three laminates considered.
In Figure 12 the elastic calculations show a reduction in wing mass for high AR conventional wings and an increase in mass for the SBW in comparison to rigid calculations. This means that the SBW does not benefit from aeroelastic loads relief as typical for swept wings. This is caused by the loads increase inboard of the strut due to the reduced torsional stiffness and increased bending stiffness (due to the strut reaction).
The optimization results for aluminum construction show an increase in wing mass at high AR for both SBW and conventional concepts in comparison to rigid and elastic aluminum results. This is due to the consideration of aileron reversal requirements. CFRP wings are less affected by this requirement as seen by the small penalty in the optimization results in comparison to the elastic results. For some cases there is a reduction in the optimized wing mass in comparison to the flexible results. This is caused by changes in the skin/stringer ratio and rib spacing to reduce the wing weight.
The strut benefit in reducing the wing loads is reduced for high AR wings that are dominated by aeroelastic effects. This effect is seen by the shift in the optimum strut position to inboard stations as the

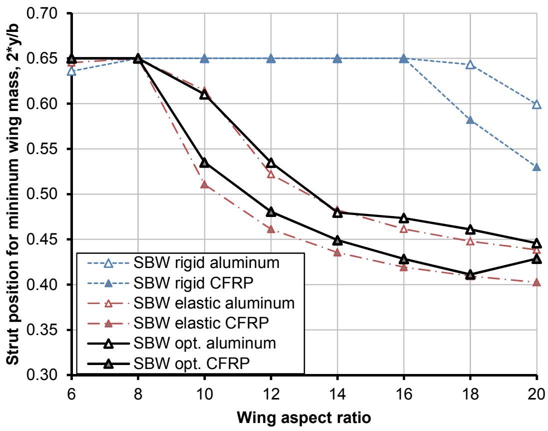

Figure 11: Strut spanwise position for minimum weight as a function of AR, material and solution sequence.

AR increases in Figure 11. If only rigid loads are considered, the optimum strut position along the span is more outboard.

The results from Figure 12 indicate that savings of 14% in the wing mass can be achieved with the SBW for a constant AR of 10 and aluminum construction. CFRP SBW wings achieve savings of 11% in comparison to an equivalent CFRP conventional wing of AR 10. Aspect ratios close to 12 of the SBW concept have the same wing mass as a conventional wing with AR=10. These benefits are related only to the wing weight. Complete aircraft "snowball" effects are likely to improve these results.

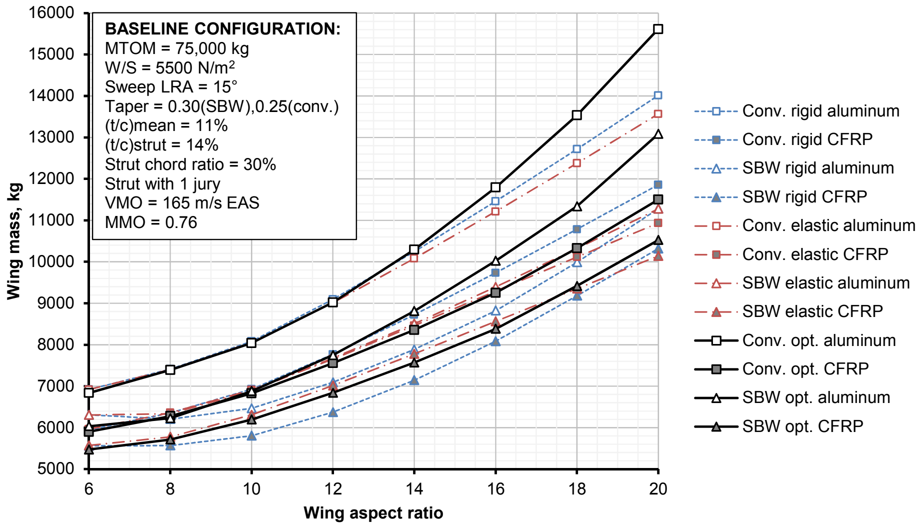

Figure 12: Wing mass as a function of AR for short range aircraft (SBW and conventional) with different calculation sequences (rigid, elastic and optimization) and materials (aluminum and CFRP). SBW results correspond to the minimum weight strut spanwise position for each case. CFRP results correspond to the minimum weight laminate.

5 CONCLUSION

The presented method enables fast answer to typical "what-if" analyses in conceptual design. The wing weight of SBW aircraft can be estimated based on strength, stability and stiffness requirements for both conventional metal and composites construction. All steps of the method are kept as simple as possible but still capturing the physics of interest. The verification results show good accuracy in comparison to more elaborate FEM and aeroelastic solvers. The design studies illustrate the flexibility and application of the method, including the potential benefits of the SBW configuration. One of the main outcomes of the design study presented is the importance to consider aeroelastic effects for the SBW concept. It is expected that the method and the discussions presented can be useful in future advanced design studies.

REFERENCES

[1] „Hurel Dubois Transports, Progress with the HD-31 and 32: the HD-45 jet project," *Flight*, p. 676, 1952.

[2] European Comission, „Flightpath 2050: Europe's Vision for Aviation," European Union, 2011.

[3] P. H. Park, "Fuel Consumption of a Strutted vs Cantilever-Winged Short-Haul Transport with Aeroelastic Considerations," *Journal of Aircraft*, vol. 17, no. 12, pp. 856-860, 1978.

[4] R. V. Turriziani, W. A. Lovell, G. L. Martin, J. E. Price, E. E. Swanson and G. F. Washburn, "Preliminary Design Characteristics of a Subsonic Business Jet Concept Employing an Aspect Ratio 25 Strut-Braced Wing," NASA CR-159361, Hampton, 1980.

[5] P. M. Smith, J. DeYoung, W. A. Lovell, J. E. Price and F. G. Washburn, "A Study of High-Altitude Manned Research Aircraft

Employing Strut-Braced Wings of High-Aspect-Ratio," NASA CR-159264, Hampton, 1981.

[6] C. E. Jobe, R. M. Kulfan and J. D. Vachal, "Wing Planforms for Large Military Transports," AIAA Paper 78-1470, Los Angeles, 1978.

[7] A. H. Naghshineh-Pour, "Structural Optimization and Design of a Strut-Braced Wing Aircraft," MSc. Thesis, Virginia Polytechnic Institute and State University, Blacksburg, 1998.

[8] O. Gur, M. Bhatia, W. H. Mason, J. A. Schetz, R. K. Kapania and N. Taewoo, "Development of a framework for truss-braced wing conceptual MDO," *Structural and Multidisciplinary Optimization,* vol. 44, pp. 277-298, 2011.

[9] M. K. Bradley and C. K. Droney, "Subsonic Ultra Green Aircraft Research: Phase I Final Report," NASA/CR-2011-216847, Hunntington Beach, 2011.

[10] M. K. Bradley and C. K. Droney, "Subsonic Ultra Green Aircraft Research Phase II: N+4 Advanced Concept Development," NASA/CR-2012-217556, Hunntington Beach, 2012.

[11] G. Carrier, O. Atinault, S. Dequand, J.-L. Hantrais-Gervois, C. Liauzun, B. Paluch, A.-M. Rodde and C. Toussaint, "Investigation of a Strut-Braced Wing Configuration for Future Commercial Transport," in *28th International Congress of the Aeronautical Societies*, Brisbane, 2012.

[12] E. M. Greitzer, P. A. Bonnefoy, E. D. l. R. Blanco, C. S. Dorbian and M. Drela, "N+3 Aircraft Concept Designs and Trade Studies, Final Report Volume 2: Appendices—Design Methodologies for Aerodynamics, Structures, Weight, and Thermodynamic Cycles," NASA/CR-2010-216794-VOL2, 2010.

[13] L. J. Hart-Smith, "The Ten-Percent Rule for Preliminary Sizing of Fibrous Composite Structures," SAWE Paper 2054, Hartfold, 1992.

[14] „Certification Specifications and Acceptable Means of Compliance for Large Aeroplanes CS-25," European Aviation Safety Agency, 2012.

[15] K. G. Pratt, "A Revised Formula for the Calculation of Gust Loads," NACA TN-2964, Washington, 1953.

[16] E. Torenbeek, Synthesis of Subsonic Airplane Design, Delft: Delft University Press, 1982.

[17] L. M. Nicolai and G. E. Carichner, Fundamentals of Aircraft and Airship Design: Volume 1 - Aircraft Design, Reston: American Institute of Aeronautics and Astronautics, Inc., 2010.

[18] O. Schrenk, "Ein einfaches Näherungsverfahren zur Emittlung von Auftriebsverteilungen längs der Tragflügelspannweite," Aerodynamischen Versuchsanstalt, Göttingen, 1940.

[19] H. Schlichting and E. Truckenbrodt, Aerodynamik des Flugzeuges, 2nd ed., Berlin/Heidelberg: Springer-Verlag, 1969.

[20] F. R. Shanley, Weight-Strength Analysis of Aircraft Structures, 2nd ed., New York: Dover Publications, Inc., 1952.

[21] G. P. Chiozzotto, „A modular implementation of aircraft simplified loads methods for conceptual design and variable fidelity processes," in *62. Deutscher Luft- und Raumfahrtkongress*, Stuttgart, 2013.

[22] D. J. Farrar, "The Design of Compression Structures for Minimum Weight," *The Journal of the Royal Aeronautical Society,* vol. LIII, pp. 1041-1052, 1949.

[23] R. Tetlow, "Design Charts for Carbon Fibre Composites," Cranfield Institute of Technology Memo No. 9, Cranfield, 1970.

[24] R. L. Bisplinghoff, H. Ashley and R. L. Halfman, Aeroelasticity, New York: Dover Publications Inc, 1996.

[25] MSC.Software Corporation, „Nastran 2010," MSC.Software Corporation, Santa Ana, CA, 2010.

[26] Introduction to Aircraft Weight Engineering, Los Angeles: Society of Allied Weight Engineers, Inc., 2007.

[27] E. Torenbeek, "Development and application of a comprehensive, design-sensitive weight prediction method for wing structures of transport category aircraft," TU Delft Report LR-693, Delft, 1992.

[28] M. Ardema, A. P. Patron, A. Hahn, H. Miura and M. D. Moore, "Analytical Fuselage and Wing Weight Estimation of Transport Aircraft," NASA TM-110392, Moffett Field, 1996.

[29] F. Dorbath, L. van Veen and U. Gaida, "Wing Secondary Structure Large Civil Jet Transport (MTOM > 40t) Statistical Mass Estimation," LTH MA 501 22-06, 2012.

[30] L. Jenkinson, P. Simpkin and D. Rhodes, "Civil Jet Aircraft Design - Aircraft Data File," Butterworth-Heinemann, 2001. [Online]. Available: http://booksite.elsevier.com/9780340741528/appendices/data-a/default.htm. [Accessed 01 06 2015].

[31] Luftfahrttechnisches Handbuch, Stand 2008, "Band Massenanalyse," Luftfahrttechnisches Handbuch, 2008.

[32] S. Bruner, S. Baber, C. Harris, N. Caldwell, P. Keding, K. Rahrig and L. Pho, "NASA N+3 Subsonic Fixed Wing Silent Efficient Low-Emissions Commercial Transport (SELECT) Vehicle Study," NASA/CR-2010-216798, 2010.

[33] J. C. Ekvall and C. F. Griffin, "Design Allowables for T300/5208 Graphite/Epoxy Composite Materials," *Journal of Aircraft,* vol. 19, no. 8, pp. 661-667, 1982.